Showcasing research from the Environmental Molecular Sciences Laboratory (EMSL), a U.S. Department of Energy, Office of Science National User Facility. Cover image created by Stephanie King, Pacific Northwest National Laboratory

An activity-based probe library for identifying promiscuous amide hydrolases

A fluorogenic substrate library was developed to visualize amide hydrolase activity in soil-derived chitin-degrading bacteria. Lead compounds were converted into activity-based probes for chemoproteomic enrichment, enabling identification of hydrolases with potential substrate promiscuity and applications in enzymatic depolymerization of synthetic and natural polyamides.

Image reproduced by permission of Battelle Memorial Institute, *Chem. Comm.*, 2025, **61**, 17846.

Image created by Stephanie King, Pacific Northwest National Laboratory

As featured in:

See Kristoffer R. Brandvold, Sankarganesh Krishnamoorthy *et al.*, *Chem. Commun.*, 2025, **61**, 17846.

ROYAL SOCIETY OF CHEMISTRY

rsc.li/chemcomm

Registered charity number: 207890

ChemComm

COMMUNICATION

View Article Online
View Journal | View Issue

Cite this: *Chem. Commun.*, 2025, **61**, 17846

Received 22nd July 2025,
Accepted 25th September 2025

DOI: 10.1039/d5cc04162g

rsc.li/chemcomm

An activity-based probe library for identifying promiscuous amide hydrolases

Chathuri J. Kombala,[a] Jared O. Kroll,[a] Lucas C. Webber,[a] Stephen J. Callister,[a] Natalie C. Sadler,[a] Erin L. Bredeweg,[b] Irlanda N. Medrano,[b] Kristoffer R. Brandvold *[a] and Sankarganesh Krishnamoorthy *[b]

A fluorogenic substrate library was developed to detect amide hydrolase activity in soil-derived chitin-degrading bacteria. Hit compounds were converted into pull-down probes for chemoproteomic enrichment, identifying previously unannotated proteins now linked to putative hydrolases. This approach prioritizes candidate hydrolases for further experimental validation with potential applications in the environment, biomanufacturing, and medicine.

Cell phenotype is the result of the complex outward expression of many underlying proteins, whose activity is influenced by abundance, post-translational modifications, co-factors and other regulatory mechanisms. While transcriptomics or proteomics provide insight into abundance, they often fail to distinguish active proteins from inactive ones. Thus, there is a need for complementary methods to understand their functional contribution to phenotype.[1,2] Furthermore, incomplete genomic annotation poses challenges in linking proteins to specific cellular processes or phenotypes.

Chemical probes are perfectly suited to bridge some of these gaps.[3] Fluorogenic synthetic substrates have been used to report on biochemical functions, even in cases where the underlying biochemistry is poorly understood.[4] For example, a library of fluorogenic ester substrates with varying fatty acid side chains was used to explore the lipidomic diversity[5] and global substrate specificity of the key amide hydrolase of *M. tuberculosis*.[6] Amide-based probes with either natural or unnatural amino acids were used to fingerprint aminopeptidases[7,8] and peptide-based[9] fluorogenic libraries have also been used to fingerprint aminopeptidase activity in *Plasmodium*. Similarly, a recently created library based on natural and unnatural amino acids was used to distinguish early-stage pancreatic tumors based on activity profiles.[10] A library-based approach has also been used to discover novel biomarkers for tumor cells[11] and IBD[12] based on aminopeptidase and protease activity. Inspired by this approach, we sought to apply a larger library of amide-based probes to characterize amino peptidases involved in nitrogen and carbon utilization pathways in soil microbes.

As with the other approaches referenced above, we drew inspiration from substrate activity screening (SAS), a mechanism-based method that uses non-natural fluorogenic substrates to identify novel enzyme acitivity.[13] SAS centers on an enzymatic cleavage reaction, such as amide bond hydrolysis,[14] and employs a library of small molecules that release a fluorescent product after enzymatic cleavage. These libraries can be screened against biological samples to uncover unique biochemical processes. SAS has been successfully applied to proteases,[14,15] phosphatases,[16] and kinases,[17] and holds potential to discover enzymes relevant to energy, biofuels and materials, and environmental and host-associated microbial processes, including hydrolases, lipases, DNases, RNases, and oxidases.[18]

SAS has several advantages over conventional high throughput screening approaches. Since a positive result requires a functionally active enzyme, false positives cannot arise from common screening artifacts such as compound aggregation, protein precipitation, or non-specific ligand binding. It is particularly effective for detecting weak-binding hits because the assay signal accumulates as a result of continuous enzyme activity. SAS's one-step synthesis greatly simplifies the generation of diverse libraries to maximize coverage of the chemical space. Furthermore, we can convert selective substrates identified through SAS into activity based probes (ABPs),[15] enabling identification of the proteins linked to the observed enzyme activity.

For the initial demonstration of the capability of SAS, we explored amide hydrolysis activity in soil-derived bacteria as they live in complex environments with diverse chemical exposure and release enzymes that can break down a wide range of compounds (Fig. S1). These microbes employ a broad spectrum of amide hydrolases, such as proteases, hydrolases and carboxypeptidases, that are relevant to nutrient cycling,[19] nitrogen access from complex plant substrates,[20] and waste recycling.[21]

[a] *Biological Sciences Division, Pacific Northwest National Laboratory, Richland, Washington 99352, USA. E-mail: krbrandvold@gmail.com*
[b] *Environmental Molecular Sciences Division, Pacific Northwest National Laboratory, Richland, Washington 99352, USA. E-mail: sankarganesh.krishnamoorthy@pnnl.gov*

The genomic profiles of soil-derived bacteria strains *Sinorhizobium meliloti* (SRB) and *Sphingopyxis fribergensis* (SPX) have identified numerous uncharacterized amidase-like domains, including chitin metabolism genes, and the majority of these genes such as, chitinase, *N*-acetylhexaminidase and deacetylase, belong to the hydrolase enzyme class.[22] They have been studied for their unique catalytic potential[23,24] and identified as a key community member of model soil consortia in recalcitrant biomass degradation. Thus, we specifically interrogated enzymatic activity from SRB and SPX, which are capable of hydrolyzing chitin/*N*-acetylglucosamine (NAG) to glucosamine.[22] We hypothesized that amide hydrolases associated with the chitin/NAG-degrading phenotype would show greater activity with NAG as the sole carbon source than with glucose.

To test our hypothesis, we used a SAS strategy to design a non-natural fluorogenic substrate library to investigate non-canonical amidase activity across structurally diverse carboxylic acid substrates (Fig. 1). The library was composed of a set of carboxylic acids purchased from ChemBridge, amino acids, and various other readily accessible carboxylic acids. To strategically capture proteases—as they are known to react with amino acid-based substrates—and set a baseline, substrates based on cationic and lipophilic amino acids were included. The anionic amino acids were excluded as they were not amenable for one-step amide coupling. The amide coupling of the library with rhodamine resulted in primarily di-amides and occasionally mono-amides. In total, there were 99 di-amides and 22 mono-amides and both subsets included aliphatic and aromatic substrates (Fig. 1A and B). The library has a molecular weight range of 444–1277, with a mean molecular weight of 789 + 182 (Fig. 1C). Lipophilicity varied greatly for the library, with clogP values ranging from 0.2–14.6, with a mean value of 7.3 + 2.8 (Fig. 1D and E). The amino acid subset clustered as more polar, the organic subset as less polar, and the ChemBridge set was more varied. We first tested our library through co-incubation with the selected SRB and SPX strains with a glucose carbon source and compared fluorescence evolution relative to buffer controls. In SRB, we observed an appreciable spread of activity for each of the three designated substrate classes (Fig. 2A), whereas most SAS probes with high turnover for the SPX strain were primarily amino acid conjugates (Fig. 2B). We further examined structural

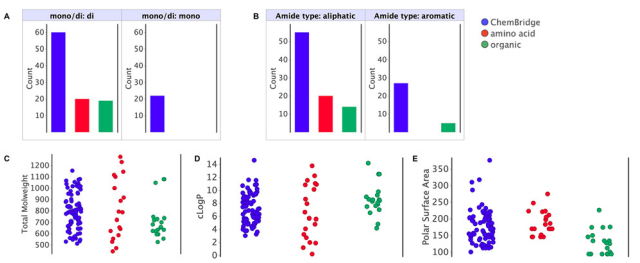

Fig. 1 Calculated properties for the substrate activity screening library. (A) Total count for each general category. (B) Count for each category by amide type. (C) Jitter plot for molecular weights for all compounds. (D) Jitter plot for clogP of all compounds. (E) Jitter plot for the calculated TPSA for all compounds.

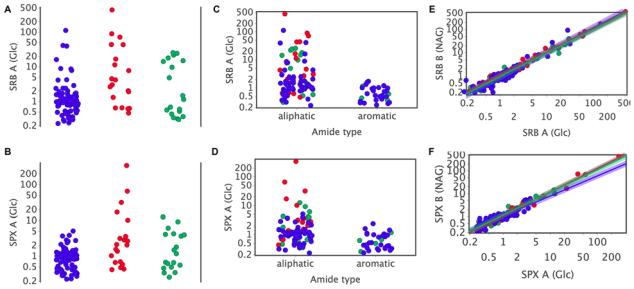

Fig. 2 Global evaluation of amidase activity for SRB (A, C, E) and SPX strains (B, D, F) by assigned substrate class and aliphatic/aromatic class. The axes are fold change of RFU SRB (or SPX)/RFU buffer. The colours indicate substrate sub-group; Blue-ChemBridge library, Red-Amino acids, Green-organic.

features that might influence activity, and found a broad range of activity for aliphatic substrates, but did not find any activity with aromatic substrates (Fig. 2C and D) for both strains, suggesting that the strains will not yield any interesting candidates for aramid degradation. Next, we tested whether there would be any shifts in activity for the respective strains upon shifting from Glu-media to NAG-media, and no major changes in substrate activity were observed for either strain (Fig. 2E and F). There were no examples where there was activity in NAG-media, but not in Glu-media. Furthermore, there were many instances in both strains of lower activity when switching from Glu-media to NAG-media. Perhaps unsurprisingly, for both strains in either media condition, the most active substrate was an amino acid derivative (Arg).

To identify structural trends, the library was analysed by focusing on amino acid-related compounds similar to the active SAS22 substrate (Fig. 3 and Fig. S2). A basic group alone did not guarantee robust activity, as lysine derivative SAS19 exhibited very low activity, and the des-amino counterpart SAS49 was completely inactive. However, the glycine-based substrate SAS44 demonstrated good activity. The loss of activity in SAS51 after acetylation of the glycine amine suggests that basicity is crucial for this compound. Additionally, increasing the side chain bulk (SAS43 and SAS48) appears to reduce activity.

Several compounds structurally similar to the highly active SAS46, a phenylalanine derivative (Fig. 3 and Fig. S3), demonstrated activity. The hydroxylated substrate (tyrosine derivative SAS47) retained 80% activity, while the des-amino compound

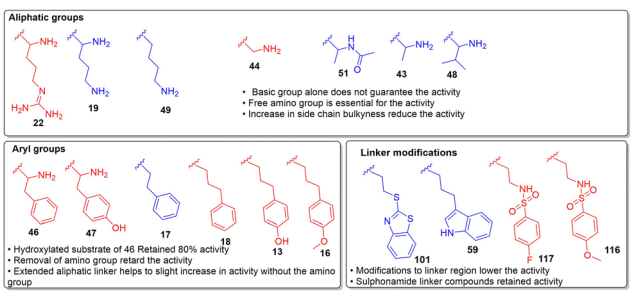

Fig. 3 Structure activity relationships (SARs) of substrate classes with aliphatic amino acid, aryl compound and different linker-related amidase activity in the SRB and SPX strains: red: high activity, blue: low activity.

SAS17 maintained 5% activity despite the removal of the amino group. Adding a methylene group to the aliphatic linker of SAS17, as in SAS18, partially restored the activity (Fig. S4). Phenyl compounds with a *p*-hydroxy (SAS13) or *p*-methoxy (SAS16) substituent showed slight increases in activity. Remarkably, SAS16, which does not mimic any natural amino acid, retained nearly 30% of the activity of the most active natural amino acid substrates. Further analysis revealed that the phenyl ring of SAS18 could be replaced with a saturated cyclohexane ring (SAS11) without losing activity, and three heterocycles at this position (SAS10, SAS12, SAS14) also displayed modest activity (Fig. 3 and Fig. S4). Modifications to the linker region of the heterocycle compounds (SAS101, SAS59) reduced activity, while sulfonamide-containing linker compounds (SAS116, SAS117) retained modest activity (Fig. 3 and Fig. S4). Observing activity across such diverse and unconventional substrates highlights the library's potential to uncover unexpected functional capabilities, opening new avenues for exploration. To identify unique probe substrates specific to the strain, the activities of all probes were compared between the two strains. Three non-canonical amidase substrates (SAS121, SAS122, and SAS126) showed a much higher preference to be turned over by SRB than SPX, regardless of the media conditions (Fig. S5). The enzymes in SRB displaying distinct activity were investigated as potential markers to differentiate this strain from SPX.

To identify enzymes responsible for activity in SRB, we converted initial substrate hits into activity-based probes (ABPs) for activity-based protein profiling (ABPP). ABPP is a powerful technique for studying enzyme activities in complex biological systems using ABPs—chemically designed molecules that selectively target and label enzymes based on their catalytic activity.[25] ABPs consist of a reactive group that covalently modifies an enzyme's active site and a reporter moiety for detection and identification.

We selected SAS122 based on its strong activity in SRB and minimal activity in SPX (73.0- and 1.1-fold increase relative to buffer controls, respectively). SAS35 was chosen as a comparison substrate because it exhibited consistently low activity in both strains (3-fold increase relative to buffer controls), serving as a control for non-specific background labelling. ABPP probes were synthesized by replacing the rhodamine fluorophore in each substrate with a chloroisocoumarin warhead. This covalent warhead binds by allowing a nucleophilic residue in the enzyme's active site to attack the carbonyl group of the isocoumarin, eliminating chloride and forming quinone methide, which can trap a second nucleophilic residue or solvent molecule in the active site. The chloroisocoumarin warhead was synthesized using previously reported methods,[26] and methyl valeric acid was conjugated to it *via* peptide coupling with HATU, yielding ABP-35 (Fig. 4). For ABP-122, carboxylic acid synthesis involved refluxing 5-chloro-2-methoxyaniline with succinic anhydride at 80 °C, followed by peptide coupling with HATU (Fig. 4A). To identify probe targets, proteins modified by ABP-122 and ABP-35 were characterized using liquid chromatography-tandem mass spectrometry (LC-MS/MS). SRB cell lysates grown in NAG media were treated with each probe or vehicle (DMSO), followed by

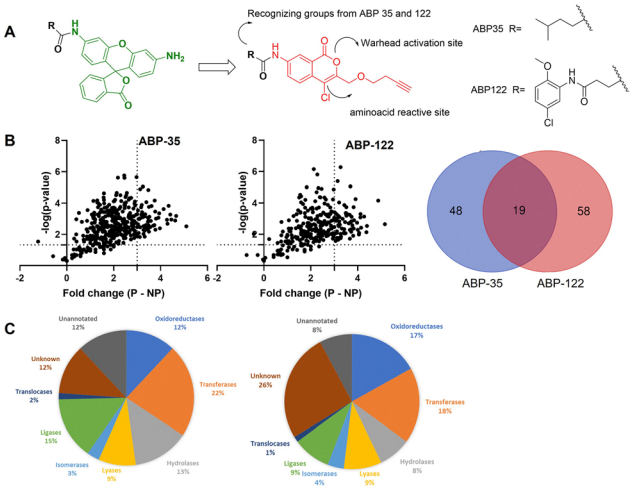

Fig. 4 ABPP provides information about functionally enriched proteins using the ABP-35 probe. (A) Conversion of screen hits to activity-based probes (left-35ABP, right-122ABP). (B) Probe-labeled proteins compared across SRB cell lysates grown on NAG media. (C) 48 and 58 proteins showed preferential enrichment for ABP-35 and ABP-122, respectively, in NAG-media. (C) EC number analysis of preferentially enriched proteins. Pie charts show the functional classifications of enriched proteins identified using ABP-35 (left) and ABP-122 B (right).

conjugation to a biotin–azide reporter tag, streptavidin-based enrichment, and proteomic analysis. Direct enrichment of probe-labeled proteins was performed with ABP-122 and ABP-35 separately, compared to DMSO-treated lysates. NAG media was selected due to higher labeling observed in fluorescence gels (Fig. S6). Proteins preferentially enriched by the probes were identified based on two criteria: (1) statistically significant differences ($p < 0.05$) between probe-labeled samples and negative controls, and (2) at least 3-fold higher abundance in probe-labeled samples compared to controls. Proteins meeting both criteria were defined as engaging in a covalent interaction (Fig. 4B). A total of 77 proteins showed activity-based enrichment with ABP-122 in NAG media compared to the no-probe control (Table S1), while 67 proteins were enriched with ABP-35 (Table S2). Among these, 19 proteins were commonly enriched by both probes, whereas 48 and 58 proteins were specifically enriched by ABP-35 and ABP-122, respectively (Fig. 4B). Enzyme commission (EC) number analysis of the identified proteins for both probes revealed preferential enrichment under defined criteria (Fig. 4C and Fig. S7). The identified proteins encompassed all functional enzyme classes, with transferases, hydrolases, oxidoreductases, lyases, and ligases being predominant. Because the warhead is activated by cleavage of the ester linkage (Fig. 4A)—whether through a catalytic residue, water mediation, or reductive cleavage—it is not surprising that broader classes of enzymes are enriched. Notably, the probes captured enzymes acting on amide bonds, including *N*-acetylglucosamine-6-phosphate deacetylase, as well as 15 unannotated proteins (Tables S1 and S2) that represent candidates for further investigation.

To understand the cellular functions associated with enriched proteins, we performed KEGG pathway analysis (Fig. S8). Comparing the representation of the enriched proteins identified using

both probes to the total predicted proteins in the SRB genome showed a significant enrichment in metabolic pathways. The overrepresentation of metabolic proteins suggests that there may be niche differences in metabolism that enable SRB to hydrolyze probes 35 and 122. Notably, amide hydrolases, which are involved in pathways such as amino acid metabolism, the urea cycle, and amino group metabolism, may be central to this metabolic activity.[27] Thus, ABP-122 has identified a distinct functional profile of amide hydrolases specific to SRB. Biosynthesis of secondary metabolites and amino sugars terms were enriched, which are terms associated with complex carbon nitrogen source utilization and processing of chitin and chitosan break down, respectively.

In summary, the SAS approach identified a unique function distinguishing two microbial species working in a consortium to degrade chitin. The probe library facilitated high-throughput identification of amide hydrolase activity in the SRB strain. Compounds 122 and 35 were identified as functional hits from the library and synthetically converted into ABPP probes, which were used in chemoproteomics to identify proteins associated with hydrolases and transferases, known for amide bond hydrolysis. KEGG pathway analysis confirmed that the probe-enriched proteins are involved in metabolic pathways. The chemoproteomics findings demonstrate the utility of the approach in prioritizing candidate proteins for further investigation of their broader hydrolase functions, which will have use in the upcycling of polyamides such as nylon.[28]

This research was financially supported on a project award (**https://doi.org/10.46936/intm.proj.2020.51699/60000258**) from the Environmental Molecular Sciences Laboratory, a DOE Office of Science User Facility sponsored by the Biological and Environmental Research program under Contract No. DE-AC05-76RL01830. PNNL is operated by Battelle for the DOE under contract DE-AC05-76RL01830.

Conflicts of interest

There are no conflicts to declare.

Data availability

The data supporting the findings in this article have been included in the supplementary information (SI). Supplementary information is available. See DOI: **https://doi.org/10.1039/d5cc04162g**.

Notes and references

1 N. C. Sadler, P. Nandhikonda, B. J. Webb-Robertson, C. Ansong, L. N. Anderson, J. N. Smith, R. A. Corley and A. T. Wright, *Drug Metab. Dispos.*, 2016, **44**, 984–991.
2 C. Buccitelli and M. Selbach, *Nat. Rev. Genet.*, 2020, **21**, 630–644.
3 K. T. Barglow and B. F. Cravatt, *Nat. Methods*, 2007, **4**, 822–827.
4 L. Tian, Y. Yang, L. M. Wysocki, A. C. Arnold, A. Hu, B. Ravichandran, S. M. Sternson, L. L. Looger and L. D. Lavis, *Proc. Natl. Acad. Sci. U. S. A.*, 2012, **109**, 4756–4761.
5 J. K. Lukowski, C. P. Savas, A. M. Gehring, M. G. McKary, C. T. Adkins, L. D. Lavis, G. C. Hoops and R. J. Johnson, *Biochemistry*, 2014, **53**, 7386–7395.
6 B. Bassett, B. Waibel, A. White, H. Hansen, D. Stephens, A. Koelper, E. M. Larsen, C. Kim, A. Glanzer, L. D. Lavis, G. C. Hoops and R. J. Johnson, *ACS Infect. Dis.*, 2018, **4**, 904–911.
7 M. Drag, M. Bogyo, J. A. Ellman and G. S. Salvesen, *J. Biol. Chem.*, 2010, **285**, 3310–3318.
8 A. Byzia, A. Szeffler, L. Kalinowski and M. Drag, *Biochimie*, 2016, **122**, 31–37.
9 T. R. Malcolm, K. W. Swiderska, B. K. Hayes, C. T. Webb, M. Drag, N. Drinkwater and S. McGowan, *Biochem. J.*, 2021, **478**, 2697–2713.
10 S. Sakamoto, H. Hiraide, M. Minoda, N. Iwakura, M. Suzuki, J. Ando, C. Takahashi, I. Takahashi, K. Murai, Y. Kagami, T. Mizuno, T. Koike, S. Nara, C. Morizane, S. Hijioka, A. Kashiro, K. Honda, R. Watanabe, Y. Urano and T. Komatsu, *Cell Rep. Methods*, 2024, **4**, 100688.
11 Y. Kuriki, T. Yoshioka, M. Kamiya, T. Komatsu, H. Takamaru, K. Fujita, H. Iwaki, A. Nanjo, Y. Akagi, K. Takeshita, H. Hino, R. Hino, R. Kojima, T. Ueno, K. Hanaoka, S. Abe, Y. Saito, J. Nakajima and Y. Urano, *Chem. Sci.*, 2022, **13**, 4474–4481.
12 R. Tanaka, J. Imai, H. Tsugawa, K. B. Eap, M. Yazawa, M. Kaneko, M. Ohno, K. Sugihara, S. Kitamoto, H. Nagao-Kitamoto, N. Barnich, M. Matsushima, T. Suzuki, T. Kagawa, Y. Nishizaki, H. Suzuki, N. Kamada and K. Hozumi, *Front. Microbiol.*, 2023, **14**, 1031997.
13 A. W. Patterson, W. J. Wood and J. A. Ellman, *Nat. Protoc.*, 2007, **2**, 424–433.
14 W. J. L. Wood, A. W. Patterson, H. Tsuruoka, R. K. Jain and J. A. Ellman, *J. Am. Chem. Soc.*, 2005, **127**, 15521–15527.
15 C. S. Lentz, A. A. Ordonez, P. Kasperkiewicz, F. La Greca, A. J. O'Donoghue, C. J. Schulze, J. C. Powers, C. S. Craik, M. Drag, S. K. Jain and M. Bogyo, *ACS Infect. Dis.*, 2016, **2**, 807–815.
16 T. D. Baguley, H.-C. Xu, M. Chatterjee, A. C. Nairn, P. J. Lombroso and J. A. Ellman, *J. Med. Chem.*, 2013, **56**, 7636–7650.
17 M. E. Breen, M. E. Steffey, E. J. Lachacz, F. E. Kwarcinski, C. C. Fox and M. B. Soellner, *Angew. Chem., Int. Ed.*, 2014, **53**, 7010–7013.
18 U. S. DOE, *Biological Systems Science Division Strategic Plan*, U.S. Department of Energy Office of Science, 2021.
19 P. Neemisha and S. Sharma, in *Structure and Functions of Pedosphere*, ed. B. Giri, R. Kapoor, Q.-S. Wu and A. Varma, Springer Nature Singapore, Singapore, 2022, ch. 8, pp. 173–188, DOI: **10.1007/978-981-16-8770-9_8**.
20 R. Shrestha, S.-c Kim, J. M. Dyer, R. A. Dixon and K. D. Chapman, *Biochim. Biophys. Acta, Mol. Cell Biol. Lipids*, 2006, **1761**, 324–334.
21 B. Zhu, D. Wang and N. Wei, *Trends Biotechnol.*, 2022, **40**, 22–37.
22 R. McClure, Y. Farris, R. Danczak, W. Nelson, H.-S. Song, A. Kessell, J.-Y. Lee, S. Couvillion, C. Henry, K. Jansson Janet and S. Hofmockel Kirsten, *mSystems*, 2022, **7**, e00372.
23 J. A. Bustamante, J. S. Ceron, I. T. Gao, H. A. Ramirez, M. V. Aviles, D. Bet Adam, J. R. Brice, R. A. Cuellar, E. Dockery, M. K. Jabagat, D. G. Karp, J. K.-O. Lau, S. Li, R. Lopez-Magaña, R. R. Moore, B. K. R. Morin, J. Nzongo, Y. Rezaeihaghighi, J. Sapienza-Martinez, T. T. K. Tran, Z. Huang, A. J. Duthoy, M. J. Barnett, S. R. Long and J. C. Chen, *PLoS Genet.*, 2023, **19**, e1010776.
24 M. Oelschlägel, C. Rückert, J. Kalinowski, G. Schmidt, M. Schlömann and D. Tischler, *Int. J. Syst. Evol. Microbiol.*, 2015, **65**, 3008–3015.
25 B. F. Cravatt, A. T. Wright and J. W. Kozarich, *Annu. Rev. Biochem.*, 2008, **77**, 383–414.
26 U. Haedke, M. Götz, P. Baer and S. H. L. Verhelst, *Bioorg. Med. Chem.*, 2012, **20**, 633–640.
27 B. W. Weber, S. W. Kimani, A. Varsani, D. A. Cowan, R. Hunter, G. A. Venter, J. C. Gumbart and B. T. Sewell, *J. Biol. Chem.*, 2013, **288**, 28514–28523.
28 E. L. Bell, G. Rosetto, M. A. Ingraham, K. J. Ramirez, C. Lincoln, R. W. Clarke, J. E. Gado, J. L. Lilly, K. H. Kucharzyk, E. Erickson and G. T. Beckham, *Nat. Commun.*, 2024, **15**, 1217.